






Article

Development and Characterization of Polymeric Composites Reinforced with Lignocellulosic Wastes for Packaging Applications

Muhammad Sulaiman ¹, Fahad Ali Rabbani ¹ , Tanveer Iqbal ¹, Fahid Riaz ^{2,*} , Muhammad Raashid ¹ ,
Nehar Ullah ³ , Saima Yasin ⁴, Yasser Fouad ^{5,*} , Muhammad Mujtaba Abbas ⁶  and M. A. Kalam ⁷ 

¹ Department of Chemical, Polymer and Composite Material Engineering, UET Lahore, New Campus, Kala Shah Kaku 39020, Pakistan; m.sulaiman@uet.edu.pk (M.S.); rabbanifahad@uet.edu.pk (F.A.R.); tanveer@uet.edu.pk (T.I.); engr_raashid@uet.edu.pk (M.R.)

² Mechanical Engineering Department, Abu Dhabi University, Abu Dhabi P.O. Box 59911, United Arab Emirates

³ Department of Chemical Engineering, UET Peshawar, Peshawar 25000, Pakistan; neharullah@uetpeshawar.edu.pk

⁴ Department of Chemical Engineering, UET Lahore, Main Campus, Lahore 54890, Pakistan; drsaima@uet.edu.pk

⁵ Department of Applied Mechanical Engineering, College of Applied Engineering, Muzahimiyah Branch, King Saud University, Riyadh 11421, Saudi Arabia

⁶ Department of Mechanical Engineering, UET Lahore, New Campus, Kala Shah Kaku 39020, Pakistan; m.muftaba@uet.edu.pk

⁷ School of Civil and Environmental Engineering, FEIT, University of Technology Sydney, Sydney, NSW 2007, Australia; mdabul.kalam@uts.edu.au

* Correspondence: fahid.riaz@adu.ac.ae (F.R.); yfouad@ksu.edu.sa (Y.F.)

Abstract: In this work, the effects of different fiber loadings on the mechanical properties of the composites at the sub-micron scale were studied through nanoindentation followed by physical characterization. The composites were prepared by incorporating different loadings of wheat straw, corn stalk, and rice husk in polypropylene copolymer using a melt processing method followed by thermal-hydraulic compression technique. Nanoindentation experiments in quasi-continuous stiffness mode were performed on the surfaces of produced composites to study the composites' elastic modulus, hardness, and creep properties. The obtained results expressed the in-depth study of the micro- and macro-level structure and behavior of particle interactions. The findings demonstrated that observable shifts in composites' hardness, elastic modulus, and creep rate had occurred. The WS-reinforced biocomposite sheet showed the highest elastic modulus of 1.09 and hardness of 0.11 GPa at 40 wt% loading in comparison to other loadings. An impact strength of 7.55 kJ/m² was noted for the biocomposite at 40 wt% RH loading. In addition, optical microscopy, Fourier transform infrared spectroscopy, water absorption, thickness swelling, and Vicat softening point studies were conducted on biocomposite sheets to evaluate differences in physical, mechanical, and thermal properties. The outstanding mechanical performance of the newly developed composites makes them suitable for use as a biodegradable packaging material.

Keywords: agricultural waste; nanoindentation; polymer; softening point; Izod impact strength; water absorption



Citation: Sulaiman, M.; Rabbani, F.A.; Iqbal, T.; Riaz, F.; Raashid, M.; Ullah, N.; Yasin, S.; Fouad, Y.; Abbas, M.M.; Kalam, M.A. Development and Characterization of Polymeric Composites Reinforced with Lignocellulosic Wastes for Packaging Applications. *Sustainability* **2023**, *15*, 10161. <https://doi.org/10.3390/su151310161>

Academic Editor: Marko Vinceković

Received: 20 April 2023

Revised: 8 June 2023

Accepted: 8 June 2023

Published: 27 June 2023



Copyright: © 2023 by the authors. Licensee MDPI, Basel, Switzerland. This article is an open access article distributed under the terms and conditions of the Creative Commons Attribution (CC BY) license (<https://creativecommons.org/licenses/by/4.0/>).

1. Introduction

Composite polymeric materials are a trendy type of new materials that consist of two or more distinct chemical and physical phases [1]. The polymeric materials have relatively lower density than metals, and hence can be tailored into a variety of shapes and applications with lower weights, higher strengths, and corrosion resistance [2,3]. Packaging is a vast global sector with links to food, medicine, family, and practically every type of

business. Ideal packing is safe, cheap, antimicrobial, sustainable, and environmentally friendly [4]. The demand for packaging has always been on the rise [5]. Most traditional packaging materials such as polyethylene, polystyrene, polypropylene, and polyethene terephthalate are fossil-fuel-based and therefore are neither environmentally friendly nor sustainable. Therefore, the use of bio-based packaging material is on the rise as concerns for the environment grow, and this market is expected to grow to 9 billion USD by 2025 [6]. PPCOs are increasingly used in packaging. Engineers strive continually to make PPCO components lighter, stronger, and more affordable. Good engineering (i.e., part design) and the use of materials that give the optimum performance for the application can achieve this [7]. The combination of a polymer with a natural fiber filler, resulting in a biocomposite, is a sustainable and technically promising replacement for non-biodegradable plastics. There are three primary important variables to consider. First, a shift away from petroleum-based materials and toward renewable sources for the production of plastics, which would reduce the release of old carbon into the environment. Second, the use of natural fibers as fillers allows for the valorization of agro-based leftovers, hence minimizing the total environmental effect of the food production cycle. Overall, the usage of biocomposites composed of polymers and fillers derived from agro-wastes enables more sustainable packaging by supporting the cradle-to-grave concept and fostering the circular economy.

Lignocellulosic fibers have several benefits, including their natural abundance, low density, high specific stiffness, and biodegradability. The distinctive features of the fibers (such as shape, aspect ratio, and crystallinity) vary significantly based on their source and origin., the quality of plant sites, the age of the plant, and the extraction technique may considerably affect the final characteristics of the biocomposites. Indeed, the high hydrophilicity and thermal instability of plant fibers are their primary disadvantages when used as fillers.

Lignocellulosic biomass is composed of varying percentages of cellulose, hemicellulose, and lignin and can be obtained from agricultural wastes and forest residues [8]. Cellulose, which gives natural fibers their mechanical qualities, is arranged in microfibrils surrounded by hemicellulose and lignin. Cellulose microfibrils can be discovered as entangled microfibrils in the cell wall. Nano-crystalline domains and amorphous portions comprise their structure.

The presence of biopolymers such as cellulose and hemicellulose in biomass presents an excellent opportunity for its use as a raw material to obtain many economically viable materials [9]. Currently, a considerable amount of waste biomass is available on Earth, most of which is unutilized. Although biomass is being used in fuel, power, polymer, and various other sectors, most of the biomass remains available [10]. For example, wood waste from timber mills alone could rise to 151.5 million tons by 2030; however, the total biomass utilization in the power sector was only 45.7 million tons in 2016. Another instance is Canada, where out of the 82.4 million tons of residue production, only 27 million tons are being used for biopolymers [11]. Biomass has been recommended as a source of raw material for the development of biopolymers for packing by various researchers [12,13]. The use of lignocellulosic biomass alone is not practical, so the best option in current scenarios is to reinforce the already existing polymeric materials by the addition of biowaste material as required [14].

Bio-sourced packing is an excellent alternative to conventional packing as it reduces waste problems and workers' diseases. Cellulose-based bio-packaging has been utilized for films, cups, cutlery, plates, dishes, and egg boxes. However, the current production of bioplastics is deficient [15]. In 2020, out of the 368 million tons of plastics produced, bioplastics accounted for only 1% [16]. Rice, wheat, and maize or corn are the top three cereal crops, i.e., grasses cultivated for grain production, consumed in the world as diet staples and account for 75% of the total grain production in the world [16]. Therefore, waste from these crops is a natural choice to be used. It is also essential to test the properties of any newly developed material. The mechanical properties of polymers generally depend on their crystallinity and underlying molecular structure. Stress-strain behavior is important to con-

sider while studying mechanical properties and can be analyzed by using nanoindentation; additionally, determining elasticity and young's modulus is important [17].

In this study, waste lignocellulosic materials obtained from the three most widely cultivated cereal crops worldwide, namely, rice husk, wheat straw, and corn straw, have been used for the development of new packing material for laboratory applications by mixing polypropylene copolymer. The resulting polymeric blends have been characterized to test for useful properties, i.e., surface morphology and mechanical properties such as hardness, modulus, creep, and load-displacement behavior by a nanoindenter, FTIR spectroscopy to analyze functional groups, the Izod impact test to check impact strength, water absorption and thickness swelling test, and Vicat softening point according to ASTM D-1525.

2. Methodology

2.1. Materials and Chemicals

Commercially available polypropylene copolymer (PPCO) was purchased from Exxon Mobil (Spring, TX, USA). Three agricultural wastes (rice husk, wheat straw, and corn stalk) were collected from local fields around Lahore, Pakistan. Maleic anhydride (MA) (98%) was purchased from Unichem (Roha, India). PPCO and MA were used as purchased.

2.2. Preparation of Agricultural Waste Samples

The raw RH, WS, and CS were converted into appropriate sizes for ease of blending with the polymer. Moreover, the physical size of the fiber has a significant impact on the physical and mechanical properties of the developed biocomposite. RH, WS, and RS were crushed in an ultra-centrifuge mill and screened to obtain particle sizes of less than 1 mm, using a sieve shaker. The biomass samples were placed in a tray drier at 105 °C for 2 h to remove the moisture content. After drying, the samples were put in polythene bags for further processing.

2.3. Mixing of Biomass with Polymer

Each biomass sample was mixed with PPCO polymer and MA at a temperature of 175 °C for a time of 5 min at 100 rpm in an indigenous internal mixer. RH (30 and 40 wt% based on polymer) was added with PPCO in the mixer, step by step, in small quantities to ensure uniform mixing. MA (2 wt% based on polymer–biomass mixture) was also added because it enhances filler distribution in the matrix (polymer). Similarly, WS and CS samples were also mixed with PPCO and MA under the same processing conditions.

2.4. Fabrication of Biocomposite Sheets

The mixed samples were used to fabricate biocomposite sheets in an indigenous thermal press. An open-shaped mold was used and filled with each mixed material, ensuring that no space was left. PET sheets were placed on the top and bottom of the mold to prevent leakage of the material, and after that, the sample was covered with steel plates and finally placed in the thermal press. In the thermal press, pressure up to 10 MPa was applied at a temperature of 185 °C for 10 min. After completion of the prescribed time, the mold was cooled under pressure and removed from the thermal press at room temperature. The sheet was taken out from the mold and placed in a polythene bag for subsequent characterization. The same procedure was followed to manufacture all biocomposite sheets. Figure 1 shows the schematic representation of the fabrication of biocomposite sheets.

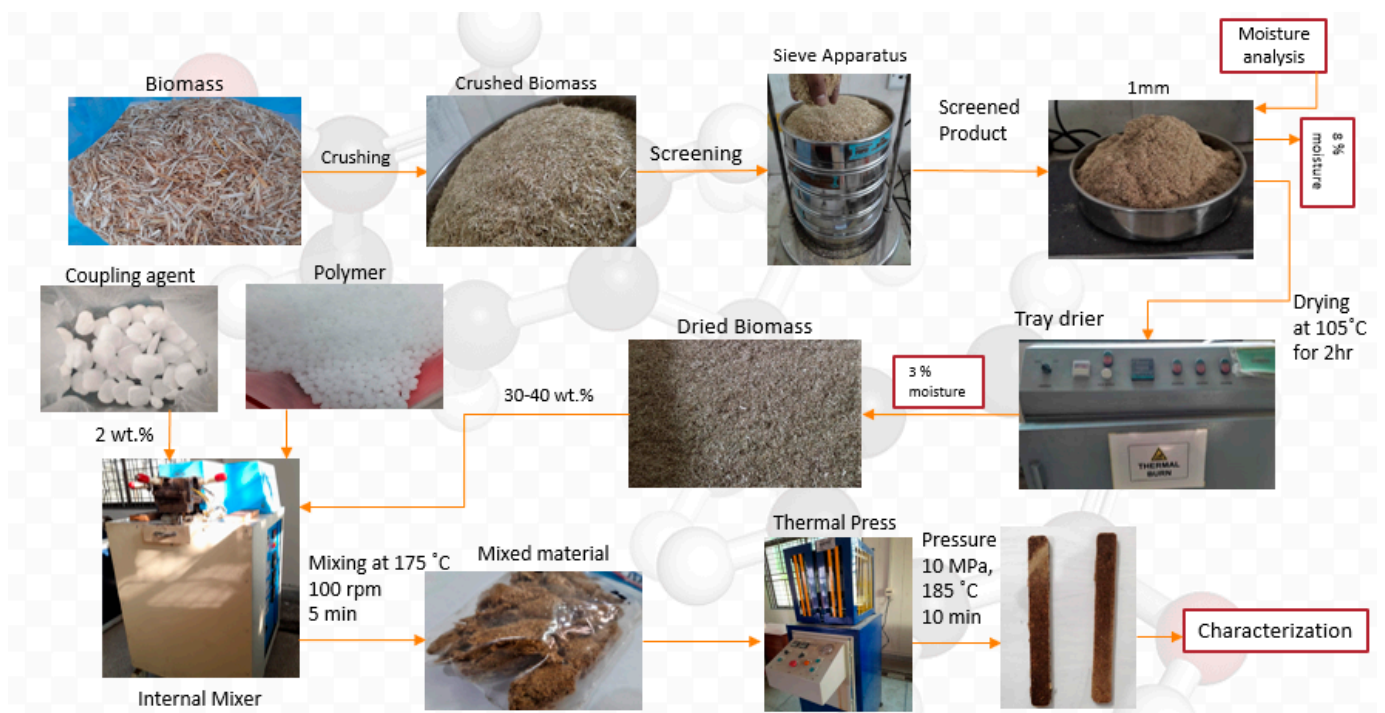


Figure 1. The schematic of agricultural residue-reinforced biocomposite development.

2.5. Characterizations

An optical microscope was used to analyze the surface morphology of the developed composite sheets. An optical microscope installed in a nanoindenter (ZwickRoell, Ulm, Germany) was used to generate optical images of 100 μm size at a magnification of 3000. FTIR spectroscopy was used to analyze functional groups present in each of the samples. Perkin Elmer Spectrum analysis with a wavelength range of 400–4000 cm^{-1} was conducted, while the Izod impact test, ASTM D-256, was performed to check the impact strength of the sheets. The dimensions of the samples were 14.5 \times 3.15 mm. The un-notch Izod impact test was conducted using a hammer weighing 0.89 kg, with a velocity of 3.105 m/s and energy of 4.315 J. Physical testing including water absorption and thickness swelling of the composites was performed. The ASTM D-570 test was conducted on each sample. After noting initial weight, each sample was placed in distilled water at room temperature (25 $^{\circ}\text{C}$) for 24, 48, and 72 h with a step size of 24 h. The samples were removed from the water, dried, and measured for weight. The percentage of water absorption was calculated by Equation (1):

$$M(\%) = \frac{M_o - M_t}{M_t} \times 100 \quad (1)$$

The percentage of thickness swelling was also calculated for each sample after a time interval of 24 h. The Vicat softening point of the composites was determined according to ASTM D-1525. A penetration depth of 1 mm and a heating rate of 120 $^{\circ}\text{C}/\text{h}$ for 2 h were employed. Nanoindentation was performed on samples of size 9 \times 3.15 mm through a nanoindenter to determine nano surface mechanical properties such as hardness, modulus, creep, and load-displacement behavior. Nanoindentation uses the contact compliance approach for data analysis, since this helps to eliminate the error introduced by the traditional hardness methodology. Using the contact compliance technique, the indentation's reaction force is determined as a function of the imposed depth.

A maximum load of 100 mN was applied to each sample at different points. Nine indents were generated through a Berkovich indenter of diamond-shaped which is installed in a nanoindenter for producing loading–unloading curves. These loading and unloading curves, called compliance curves, were used to compute hardness, modulus, and creep.

In the contact compliance mode, the actual indentation area of the sample was measured based on the indentation tip shape and the depth of penetration.

3. Results and Discussion

3.1. Surface Morphological Analysis

Figure 2a–f shows the optical surface morphology of agro-waste-reinforced biocomposites at different loadings. It can be seen from Figure 2a that surface of the composite was smoother and there was not any kind of roughness or irregularity. This could be due to smaller particle sizes and the uniform distribution of RH particles throughout the matrix phase. As fiber content increased in the biocomposite (40 wt% loading), the surface was not as smooth as compared to the composite having 30 wt% RH loading, as depicted in Figure 2b. Some fibers were mixed well with the matrix, and some were prone to the formation of irregularities at the surface. The WS biocomposite surface is shown in Figure 2c,d. The lesser content of fiber mixed well with matrix, forming good interfacial bonding, and showing a uniform surface [18]. The biocomposite (40 wt% loading) sheet is shown in Figure 3b. Increasing the fiber content showed uniform mixing and proper distribution of WS particles, resulting in good bonding as compared to the biocomposite (30 wt% loading). The CS biocomposite (30 wt% loading) sheet is shown in Figure 2e. CS fibers have a larger area per volume, so during internal mixing, the fiber was not mixed well with the matrix, leading to poor adhesion, and hence forming irregularities at the surface of the biocomposite [19]. With a greater amount of fiber CS biocomposite (40 wt% loading), there also was not a good formation of bonding between the fiber and matrix, leading to poor adhesion, resulting in more irregularities at the surface, as shown in Figure 2f.

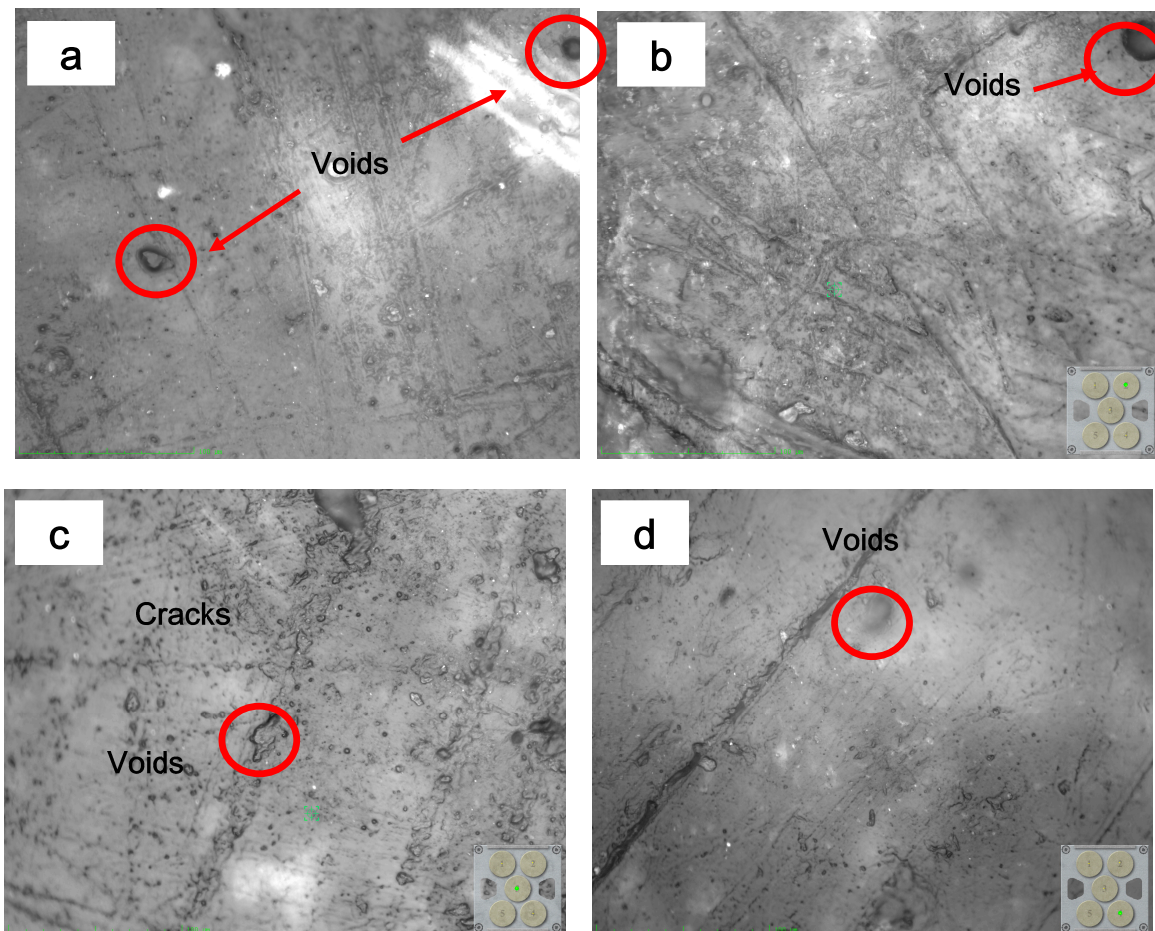


Figure 2. Cont.

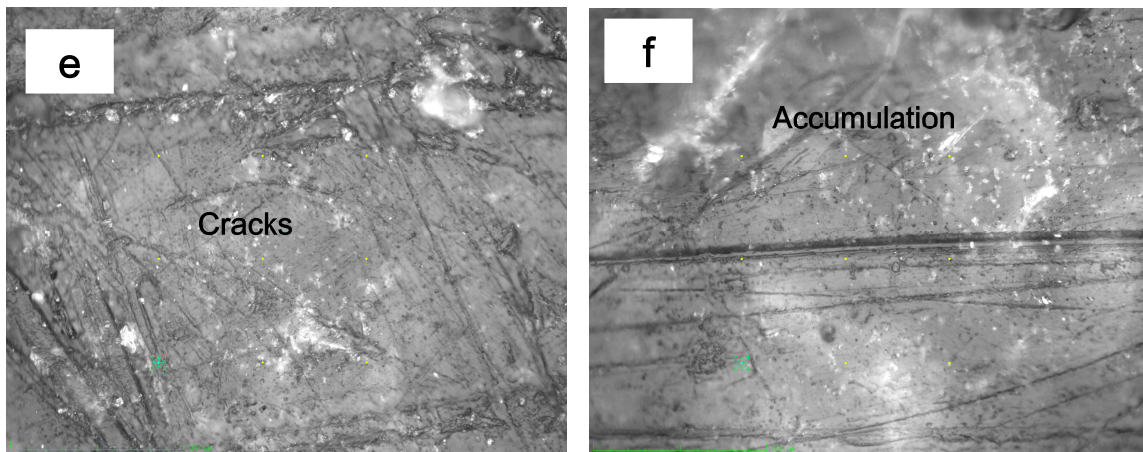


Figure 2. Surface morphology of agricultural residue-reinforced biocomposites at different loadings: (a) (30 wt% RH loading), (b) (40 wt% RH loading); (c) (30 wt% WS loading); (d) (40 wt% WS loading); (e) (30 wt% CS loading); (f) (40 wt% CS loading).

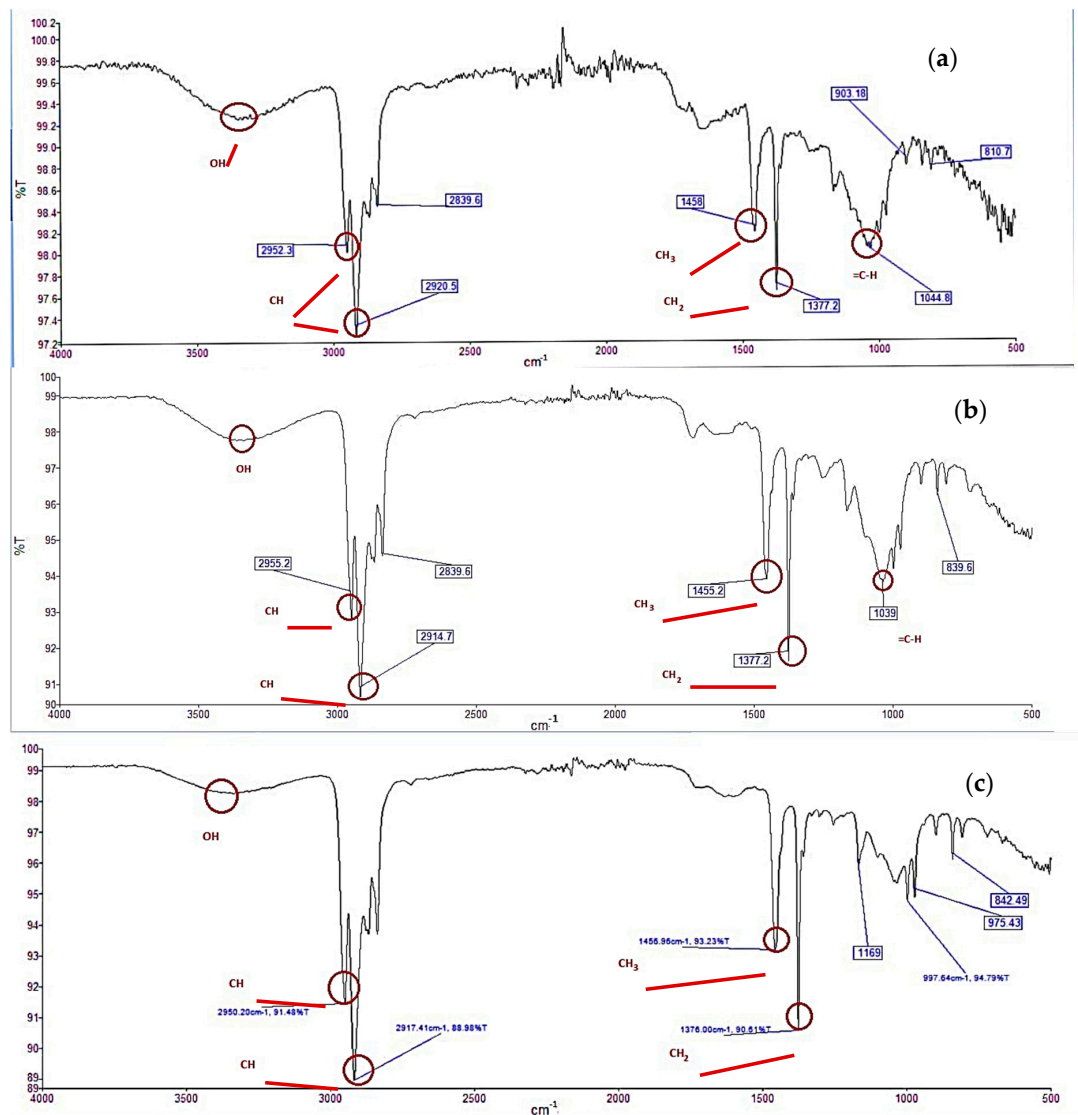


Figure 3. FTIR spectra of agricultural waste-reinforced biocomposite: (a) (RH composite); (b) (WS composite); (c) (CS composite).

3.2. Functional Group Analysis

FTIR was employed to analyze the possible types of functional groups present in the biocomposites. Wavenumbers had shifted due to mixing fiber with the matrix material. FTIR spectra of RH-, WS-, and CS-reinforced biocomposites are shown in Figure 3a–c, showing possible functional groups. The wavenumber shifts were noted at 2952, 2955, 2914, and 2839.6 cm^{-1} and may be attributed to C-H alkanes. Wavenumber shifts were noted at 1455 and 1377.2 cm^{-1} , representing $-\text{CH}_2$ and $-\text{CH}_3$ groups. Peaks at 1044.8 and 1039 cm^{-1} represent $=\text{C}-\text{H}$ groups.

3.2.1. Water Absorption and Thickness Swelling Behavior of Biocomposites

Figure 4 represents the water absorption (%) of biocomposites with intervals of 24 h. The water absorption rate decreased with increasing immersion time (24, 48, 72 h). This phenomenon might happen due to the presence of hydrophilic components (cellulose and hemicellulose) in lignocellulosic waste. Cellulose and hemicellulose promote the absorption of water depending on environmental conditions. Moreover, hydroxyl groups in cellulose and hemicellulose attract water molecules and bind with them through hydrogen bonding [20]. In addition, poor adhesion between fiber particles and polymer matrix generates void spaces around fiber particles, resulting in increased water absorption. Biocomposites are continuously exposed to moisture. Therefore, brittle thermosetting resin will experience micro-cracking due to the swelling behavior of fibers, resulting in debonding of the biocomposites [21]. Radzi et al. (2019) [16] showed the same effect on water absorption. It is evident from Figure 4 that the water absorption rate was increased with increasing biomass loading in the case of CS and RH loadings. This could be due to the presence of higher hemicellulose content. In the case of WS loading, the water absorption rate decreased with increasing loading. This phenomenon might be due to the compact structure of WS. Moreover, hydrophilic WS inside the composites can only absorb a trace amount of water because the polymer has sufficiently insulated it from water, i.e., most fibers have been encased by the surrounding polymeric material to prevent them from direct interaction with water molecules. In addition, WS composites with their structural similarities showed relatively similar water-absorbing performances for each WS loading when compared to the other composites. There is more room for water within the fibers.

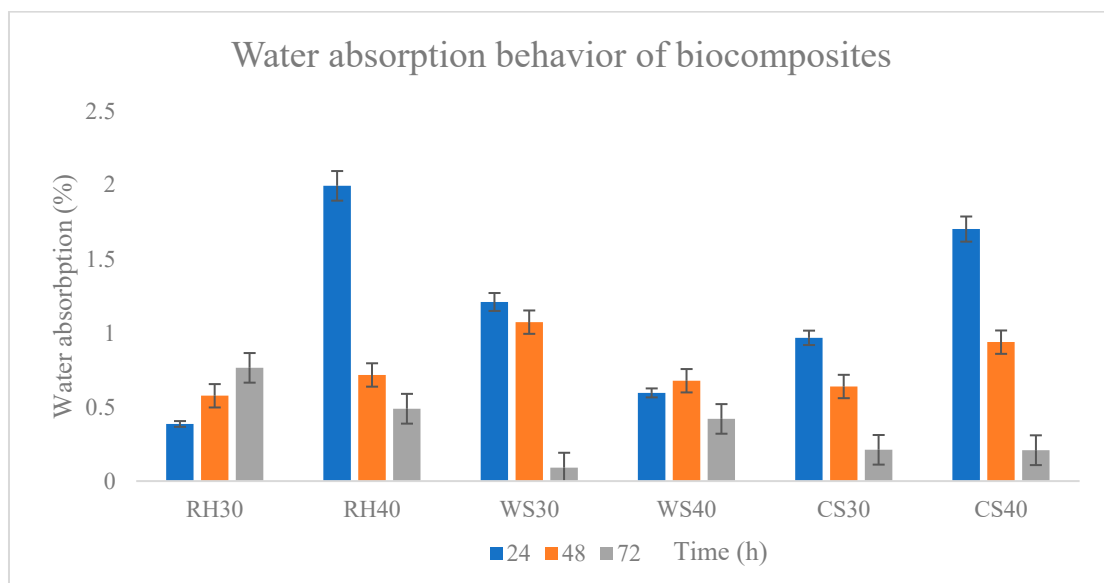


Figure 4. Water absorption behavior of agricultural residue-reinforced biocomposites at different loadings.

Figure 5 illustrates the biocomposites' thickness swelling (TS) with intervals of 24 h. It is depicted in Figure 5 that the TS of RH-reinforced biocomposite at 30 wt.% loading was less in comparison to 40 wt.% loading. This might happen due to the low biomass content, resulting in less water absorbed. It can also be inferred that bonding between fiber and matrix plays an important role. The stronger bonding indicates no voids and cracks in the sheet, resulting in less susceptibility to water damage [22]. Initially, the swelling was constant for some time, after which there was an abrupt change. In the case of the WS biocomposite with 30 wt.% loading, there was little effect on thickness compared with the RH biocomposite (30 wt.% loading). While the biomass content was increased to 40%, a noticeable change was observed in comparison with the WS biocomposite (30 wt.% loading).

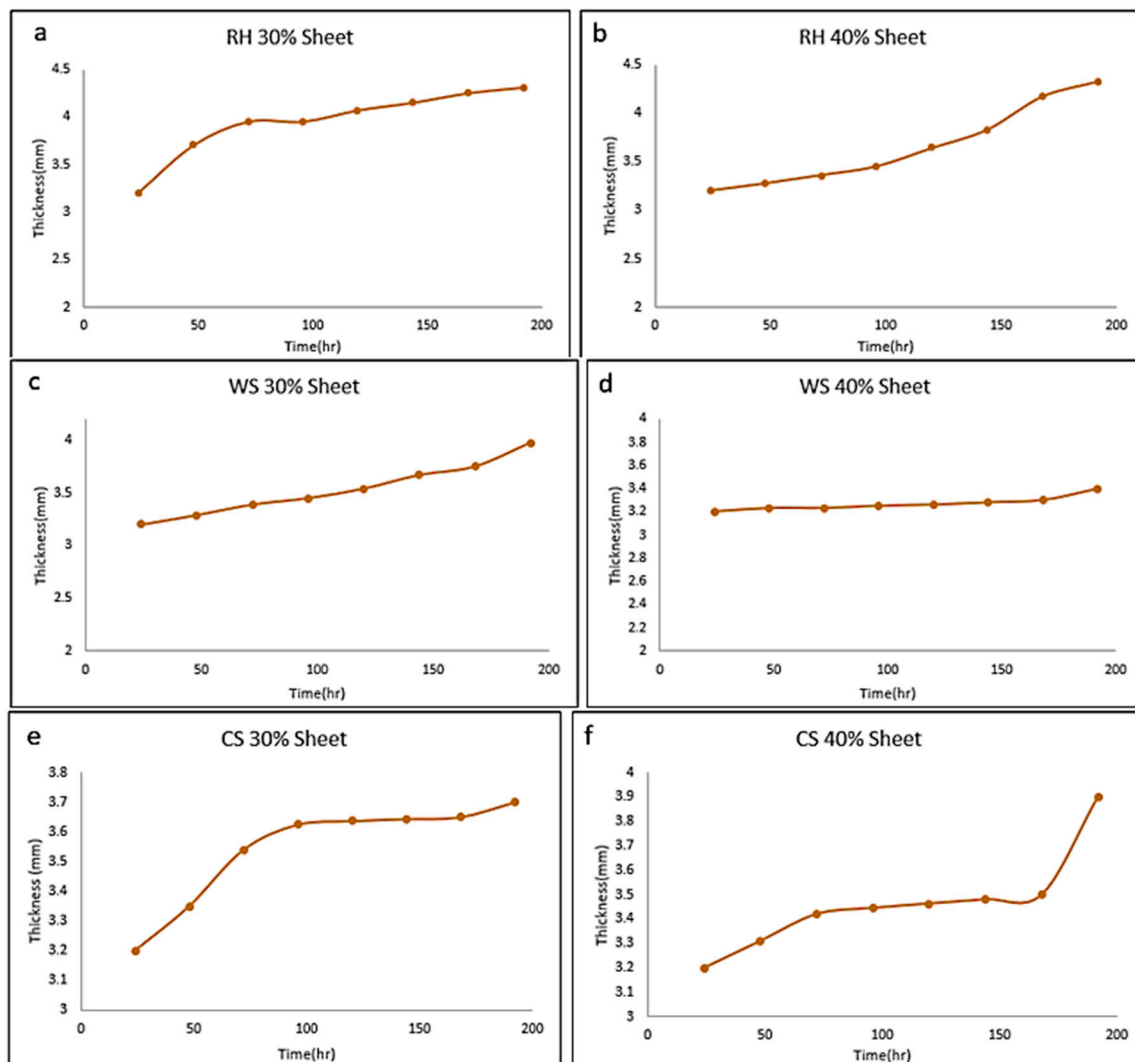


Figure 5. Thickness swelling behavior of agricultural residue-reinforced biocomposites at different loadings: (a) (30 wt% RH); (b) (40 wt% RH); (c) (30 wt% WS); (d) (40 wt% WS); (e) (30 wt% CS); (f) (40 wt% CS).

For loadings ranging from 30% to 40%, WS composites exhibited similar thickness swelling. For CS biocomposites, it can be seen in Figure 5 that for 30 and 40 wt% biomass loadings, there was no significant change. CS biocomposite 30 wt% loading, however, showed increasing swelling behavior, particularly at higher loading. CS fibers showed a large ratio of surface volume to area compared to others, leading to poor bond formation [23].

3.2.2. Impact Strength Analysis

Table 1 represents the Izod impact strength of biocomposites at different loadings (30 and 40 wt%). It is evident from the values that the CS-reinforced biocomposite showed higher impact strength compared to other composites at 30 wt% loading. This phenomenon might be due to the good interfacial adhesion of CS particles with the polymer. Moreover, the good adhesion might be due to the smaller particle size, as smaller particles showing a larger surface area per volume ultimately lead to better interfacial bonding between biomass and polymer [24]. In the case of 40 wt% loadings, the RH-based composite indicated higher impact strength compared to other composites. This may be due to the compositions and shapes of the RH particle form compared to WS and CS fibers.

Table 1. Izod impact strength values of agricultural residue-reinforced biocomposites.

Sample Name	Impact Strength (kJ/m ²) (30 wt% Loading)	Impact Strength (kJ/m ²) (40 wt% Loading)
RH biocomposite	5.8215	7.5565
CS biocomposite	7.3317	3.5313
WS biocomposite	3.5296	3.6318

Consequently, good distribution and uniform mixing of RH particles occurred throughout the polymer. It could also be concluded that the decreasing impact strength of the composites indicated the accumulation of filler particles in the polymer. As a result, weak interfacial bonding between reinforcing and substrate materials may happen, leading to poor mechanical properties of the resultant composites [25].

3.2.3. VICAT Softening Point Analysis

The softening point temperature represents the motion of the PPCO molecular chain at elevated temperatures.

The Vicat softening point relationship of the composites with various biomass loadings is shown in Figure 6. As biomass loading increased, a decline in softening point was noted in all types of composites. The Vicat softening point of pure PPCO was obtained at 151 °C [26]. It was observed that when fiber content increased, the softening temperature first increased and later decreased. Composites reinforced with agro-residue have a greater softening temperature because of particle stiffness and fiber aspect ratio. During the test, excessive temperature was recorded to speed up molecular mobility. While the stiff particle fillers may reduce the polymers' heat deformation temperature.

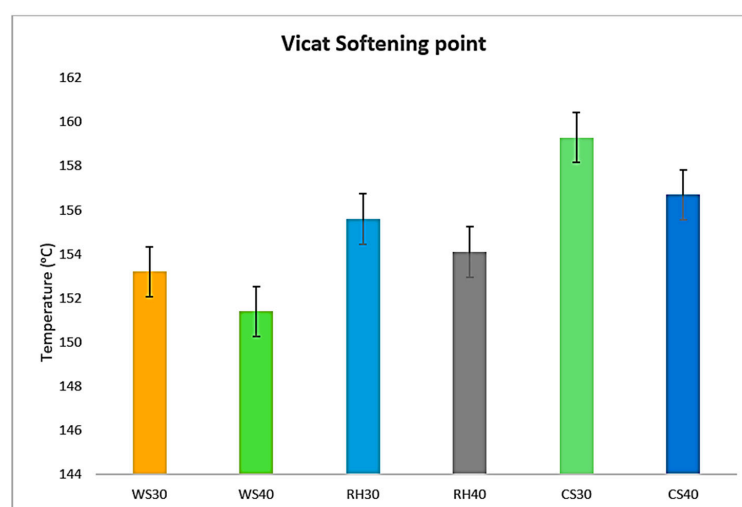


Figure 6. Vicat softening point of the agricultural residue-reinforced biocomposites at different loadings.

For a 10% rise in fiber content, the Vicat softening point decreased by 1.0%. This could be attributed to the presence of silica, resulting in improved interfacial bonding between matrix and fiber [26]. Zhang et al. (2015) [27] showed the same results. For WS- and CS-based composites, the Vicat softening point was reduced by 1.17% and 1.63%, respectively, as fiber content increased by 10 wt.%. CS biocomposites exhibited substantially higher values than others. The fibers of CS resist pressure during softening temperature. Thus, CS-based composites might be employed in applications where the temperature is high.

3.2.4. Hardness Elastic Modulus Analysis

Figure 7a,b represents the composites' hardness and elastic modulus behavior at different biomass loadings. Indentation hardness dwindled as the contact depth increased. Up to 1 μm of penetration depth, indentation hardness was continuously decreased. Onwards, it became constant until a point where indentation hardness became constant. The outer surface was hardened compared to the inner region [24]. This could have occurred because of the environmental impact on the top surface of the composites, generating hardening effects [25]. Due to the sheets' rough and uneven top surface, a wide range of hardness and elastic modulus was found. This variance may have resulted from environmental effects on the surface, inadequate identification of the top surface, or a flaw in the geometry of the indenter tip. In general, a high elastic modulus corresponds to a high degree of hardness, and vice versa.

Moreover, softer behavior may indicate the occurrence of an amorphous phase. It was also notable that the higher values of indentation hardness and modulus were not observed for materials in which fiber loading was not high. This could be due to fiber/matrix bonding resulting in improved mechanical properties. Figure 7a also shows the fabricated composites' modulus behavior as a contact depth function. Initially, higher modulus values were noted, indicating that the material was challenging, rigid, and not finished properly at the surface. The material with a high elastic modulus showed higher stiffness because of the good mechanical bonding between fiber and matrix. The WS and CS biocomposites showed significantly higher hardness and elastic modulus than the RH biocomposite. This phenomenon indicated that WS- and CS-reinforced composites have a higher tendency to resist deformation. The maximum modulus obtained was 6.9 GPa for the WS composite. Furthermore, after a contact depth of 1.5 μm , the modulus values of the samples started to decrease. It can be concluded that materials with low modulus showed higher deformation rates as per the force applied, and vice versa.

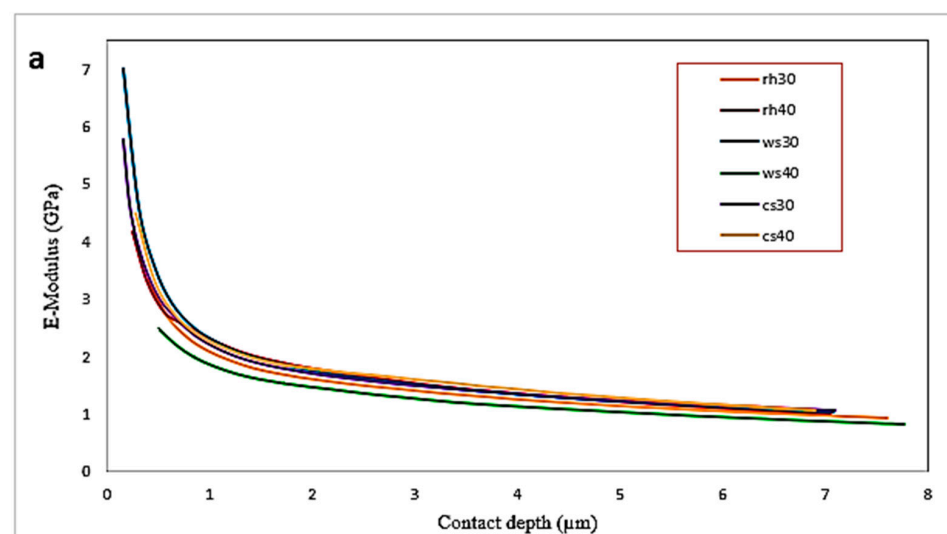


Figure 7. Cont.

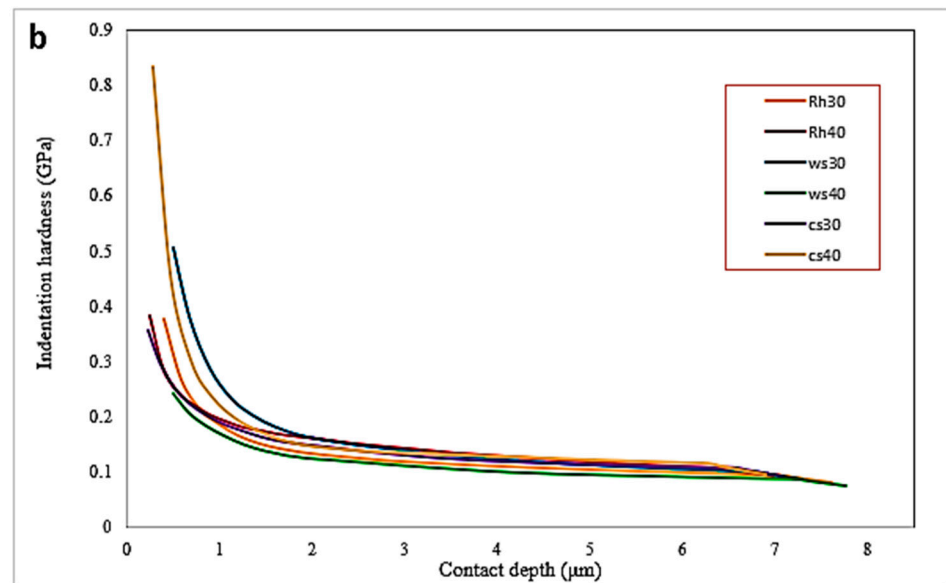


Figure 7. Indentation hardness and modulus of agricultural residue-reinforced biocomposites as a function of contact depth. (a) modulus; (b) hardness.

3.2.5. Creep Analysis

The study of creep behavior is significant for understanding material deformation during load. Due to the semi-crystalline and amorphous nature of the component particles, the biocomposites exhibited viscoelastic behavior. The major influences on the viscoelastic behavior of the composite are stress, holding time, and temperature. Figure 8 indicates the creep rate of the composites under constant load. The creep curve showed a decreasing trend as time increased. In the primary creep stage, the creep rate initiated at relatively higher values but rapidly increased with time. This phenomenon may be attributed to the change in the orientation of fiber particles under load because of slippage [14]. As the material is exposed to continuous levels of load, it may start to deform permanently. After about 9 s, creep reached a secondary stage with a steady-state continuous decrease. The CS biocomposite showed higher creep rates than the other biocomposites. Thus, interfacial adhesion was disrupted, and CS particles slipped, affecting creep resistance.

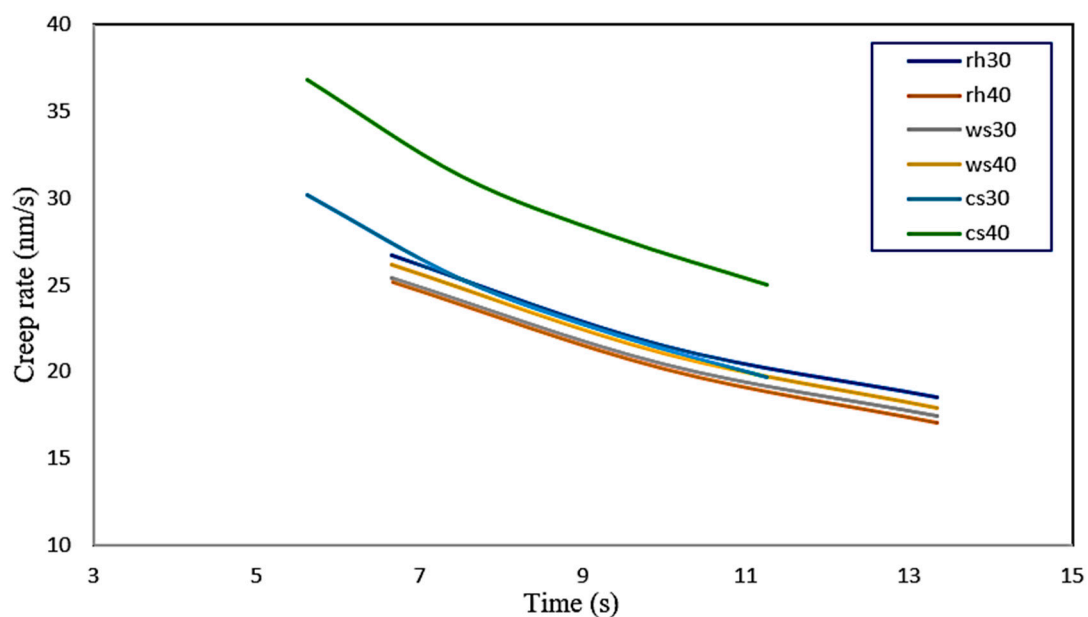


Figure 8. Creep rate of agricultural residue-reinforced biocomposites as a function of time.

4. Conclusions and Future Perspectives

In this study, the surface morphological analysis, functional group analysis, water absorption and thickness swelling behavior, and impact strength analysis of the lignocellulosic waste-based biocomposites were investigated. The optical surface morphology of the composites was smoother and showed good bonding between fiber and matrix at 30 wt% loadings. However, as the fiber content increased, the surface became less smooth due to poor adhesion between the fiber and matrix, resulting in more irregularities. The FTIR spectra of the composites showed possible functional groups and the wavenumber shifts indicated the presence of C-H alkanes, -CH₂ and -CH₃ groups, and =C-H groups. The water absorption rate and thickness swelling of the sheets increased with immersion time and biomass content due to the presence of hydrophilic components and poor adhesion between fiber particles and the polymer matrix. The impact strength analysis showed that RH- and CS-reinforced biocomposites had the highest impact strength at 40 wt%, and 30% wt.% loadings, respectively. Hardness, elastic modulus, and mechanical creep behavior were evaluated by the nanoindentation technique. The indentation hardness of the composites decreased with an increase in contact depth up to 1 μm and then became constant. The WS and CS biocomposites showed significantly higher elastic moduli than the RH biocomposite, indicating their greater tendency to resist deformation. It was found that creep behavior is the function of load applying time, and the CS biocomposite showed higher creep rates than the other biocomposites. The study provides insights into the factors affecting the properties of the fabricated biocomposites reinforced with different agricultural residues at different loadings. Due to its good mechanical characteristics, this work may give a practical way for creating load-bearing materials in packaging applications employing PPCO-bonded lignocellulosic waste-based composites.

Author Contributions: Conceptualization, M.S.; Methodology, M.S.; Software, M.R. and M.M.A.; Validation, F.A.R. and N.U.; Formal analysis, F.A.R. and M.M.A.; Writing—original draft, M.S.; Writing—review & editing, T.I., F.R., M.R., N.U., S.Y., Y.F., M.M.A. and M.A.K.; Project administration, T.I.; Funding acquisition, Y.F. All authors have read and agreed to the published version of the manuscript.

Funding: This research was funded by the Deputyship for research and innovation, “Ministry of Education” in Saudi Arabia (IFKSUOR3-273-1).

Informed Consent Statement: Not applicable.

Data Availability Statement: Data will be available on request.

Acknowledgments: The authors extend their appreciation to Deputyship for research and innovation, “Ministry of Education” in Saudi Arabia for funding this research (IFKSUOR3-273-1).

Conflicts of Interest: The authors declare no conflict of interest.

Abbreviations

RH	rice husk
WS	wheat straw
CS	corn stalk
PPCO	polypropylene copolymer
FTIR	fourier transform infrared spectroscopy
OM	optical microscopy
WA	water absorption
TS	thickness swelling
QCSM	quasi continuous stiffness mode

References

1. Aisyah, H.A.; Paridah, M.T.; Sapuan, S.M.; Ilyas, R.A.; Khalina, A.; Nurazzi, N.M.; Lee, S.H.; Lee, C.H. A Comprehensive Review on Advanced Sustainable Woven Natural Fibre Polymer Composites. *Polymers* **2021**, *13*, 471.
2. Hsissou, R.; Seghiri, R.; Benzekri, Z.; Hilali, M.; Rafik, M.; Elharfi, A. Polymer Composite Materials: A Comprehensive Review. *Compos. Struct.* **2021**, *262*, 113640. [[CrossRef](#)]
3. Kamarudin, S.H.; Rayung, M.; Abu, F.; Ahmad, S.; Fadil, F.; Karim, A.A.; Norizan, M.N.; Sarifuddin, N.; Mat Desa, M.S.; Mohd Basri, M.S.; et al. A Review on Antimicrobial Packaging from Biodegradable Polymer Composites. *Polymers* **2022**, *14*, 174. [[CrossRef](#)] [[PubMed](#)]
4. Zhang, M.; Biesold, G.M.; Choi, W.; Yu, J.; Deng, Y.; Silvestre, C.; Lin, Z. Recent Advances in Polymers and Polymer Composites for Food Packaging. *Mater. Today* **2022**, *53*, 134–161. [[CrossRef](#)]
5. Caiw, L. A review on the selection of raw Materials and reactors for biomass fast pyrolysis in China. *Fuel Process. Technol.* **2021**, *221*, 106919.
6. Mankar, A.R.; Pandey, A.; Modak, A.; Pant, K.K. Pretreatment of Lignocellulosic Biomass: A Review on Recent Advances. *Bioresour. Technol.* **2021**, *334*, 125235. [[CrossRef](#)] [[PubMed](#)]
7. Zhao, Z.; Yan, H.; Zuo, J.; Tian, Y.; Zillante, G. A Critical Review of Factors Affecting the Wind Power Generation Industry in China. *Renew. Sustain. Energy Rev.* **2013**, *19*, 499–508.
8. Dey, N.; Vickram, S.; Thanigaivel, S.; Subbaiya, R.; Kim, W.; Karmegam, N.; Govarthanam, M. Nanomaterials for Transforming Barrier Properties of Lignocellulosic Biomass towards Potential Applications—A Review. *Fuel* **2022**, *316*, 123444. [[CrossRef](#)]
9. Salins, S.S.; Reddy, S.V.K.; Kumar, S. Assessment of Process Parameters in a Dehumidification Process Using Biomass-Based Wood Shaving as a Packing Material. *Indoor Built Environ.* **2022**, *31*, 496–509.
10. Trifol, J.; Marin Quintero, D.C.; Moriana, R. Pine Cone Biorefinery: Integral Valorization of Residual Biomass into Lignocellulose Nanofibrils (LCNF)-Reinforced Composites for Packaging. *ACS Sustain. Chem. Eng.* **2021**, *9*, 2180–2190. [[CrossRef](#)]
11. Sid, S.; Mor, R.S.; Kishore, A.; Sharanagat, V.S. Bio-Sourced Polymers as Alternatives to Conventional Food Packaging Materials: A Review. *Trends Food Sci. Technol.* **2021**, *115*, 87–104. [[CrossRef](#)]
12. Jeyasri, R.; Muthuramalingam, P.; Satish, L.; Pandian, S.K.; Chen, J.-T.; Ahmar, S.; Wang, X.; Mora-Poblete, F.; Ramesh, M. An Overview of Abiotic Stress in Cereal Crops: Negative Impacts, Regulation, Biotechnology and Integrated Omics. *Plants* **2021**, *10*, 1472. [[CrossRef](#)]
13. Sulaiman, M.; Rabbani, F.A.; Iqbal, T.; Kazmi, M.A.; Yasin, S.; Mujtaba, M.; Kalam, M.; Almomani, F. Impact of eco-friendly chemical pretreatment on physicochemical and surface mechanical properties of sustainable lignocellulosic agricultural waste. *Algal Res.* **2023**, *71*, 103051. [[CrossRef](#)]
14. Rabbani, F.A.; Yasin, S.; Iqbal, T.; Farooq, U. Experimental Study of Mechanical Properties of Polypropylene Random Copolymer and Rice-Husk-Based Biocomposite by Using Nanoindentation. *Materials* **2022**, *15*, 1956. [[PubMed](#)]
15. Jawaid, M.; Alothman, O.Y.; Salit, M.S. *Green Biocomposites: Design and Applications*; Springer: Berlin/Heidelberg, Germany, 2017. [[CrossRef](#)]
16. Radzi, A.M.; Sapuan, S.M.; Jawaid, M.; Mansor, M.R. Water Absorption, Thickness Swelling and Thermal Properties of Roselle/Sugar Palm Fibre Reinforced Thermoplastic Polyurethane Hybrid Composites. *J. Mater. Res. Technol.* **2019**, *8*, 3988–3994. [[CrossRef](#)]
17. Xie, Q.; Li, F.; Li, J.; Wang, L.; Li, Y.; Zhang, C.; Xu, J.; Chen, S. A New Biodegradable Sisal Fiber–Starch Packing Composite with Nest Structure. *Carbohydr. Polym.* **2018**, *189*, 56–64. [[PubMed](#)]
18. Sukudom, N.; Jariyasakoolroj, P.; Jarupan, L.; Tansin, K. Mechanical, Thermal, and Biodegradation Behaviors of Poly(Vinyl Alcohol) Biocomposite with Reinforcement of Oil Palm Frond Fiber. *J. Mater. Cycles Waste Manag.* **2019**, *21*, 125–133. [[CrossRef](#)]
19. Asadollahzadeh, M.; Mahboubi, A.; Taherzadeh, M.J.; Åkesson, D.; Lennartsson, P.R. Application of Fungal Biomass for the Development of New Polylactic Acid-Based Biocomposites. *Polymers* **2022**, *14*, 1738.
20. Bax, B.; Müssig, J. Impact and Tensile Properties of PLA/Cordenka and PLA/Flax Composites. *Compos. Sci. Technol.* **2008**, *68*, 1601–1607.
21. Iqbal, T.; Yasin, S.; Zafar, M.; Zahid, S.; Ishteyaque, S.; Briscoe, B.J. Nanoindentation response of scratched Polymeric Surfaces. *Tribol. Trans.* **2015**, *58*, 801–806. [[CrossRef](#)]
22. Tian, S.; Li, B.; He, H.; Liu, X.; Wen, X.; Zhang, Z. Fabrication and Mechanical Properties of High-Durability Polypropylene Composites via Reutilization of SiO₂ In-Situ-Synthesized Waste Printed Circuit Board Powder. *Polymers* **2022**, *14*, 1045. [[CrossRef](#)] [[PubMed](#)]
23. Girones, J.; Lopez, J.P.; Vilaseca, F.; Bayer, J.; Franco, R.P.J.; Mutje, P. Biocomposite from musa textilis and propylene: Evaluation of flexural properties and impact strength. *Compos. Sci. Technol.* **2010**, *71*, 122–128. [[CrossRef](#)]
24. Sulaiman, M.; Iqbal, T.; Yasin, S.; Mahmood, H.; Shakeel, A. Study of Nano-Mechanical Performance of Pretreated Natural Fiber in Ldpe Composite for Packaging Applications. *Materials* **2020**, *13*, 4977. [[CrossRef](#)]
25. Sulaiman, M.; Iqbal, T.; Yasin, S.; Mahmood, H.; Shakeel, A. Fabrication and Nanomechanical Characterization of Thermoplastic Biocomposites Based on Chemically Treated Lignocellulosic Biomass for Surface Engineering Applications. *Front. Mater.* **2021**, *8*, 733109. [[CrossRef](#)]

26. Wang, J.; Euring, M.; Ostendorf, K.; Zhang, K. Biobased materials for food packaging. *J. Bioresour. Bioprod.* **2022**, *7*, 1–13. [[CrossRef](#)]
27. Zhang, Y.; Wen, B.; Cao, L.; Li, X.; Zhang, J. Preparation and properties of unmodified ramie fiber reinforced polypropylene composite. *J. Wuhan Univ. Technol.* **2015**, *30*, 198–202. [[CrossRef](#)]

Disclaimer/Publisher’s Note: The statements, opinions and data contained in all publications are solely those of the individual author(s) and contributor(s) and not of MDPI and/or the editor(s). MDPI and/or the editor(s) disclaim responsibility for any injury to people or property resulting from any ideas, methods, instructions or products referred to in the content.